

Magnetic dipole transition calculations in ^{52}Cr using the full Skyrme interaction

M. C. Barton and P. D. Stevenson

Department of Physics, University of Surrey, Guildford, Surrey, GU2 7XH, United Kingdom

Abstract. The purpose of this paper is to investigate the use of the TDHF method with different Skyrme force interactions for the prediction of the M1 strength function associated with ^{52}Cr , in particular due to the tensor part of the Skyrme force. ^{52}Cr was chosen due to the recent interest experimentally in this nucleus and the clear data available for comparison.

The method used involves applying an instantaneous boost to the wavefunction at the beginning of the dynamical calculations in order to initiate a broadband excitation of the nucleus, following which a Fourier analysis is made.

The results of the TDHF simulation found broad agreement with experiment for the range of energies which excite an M1 transition for a variety of forces. The tensor terms appear to be important in qualitatively changing the details of the strength distribution in the main part of the strength function between around 8 and 12 MeV.

1. Introduction

The time-dependent Hartree-Fock (TDHF) technique [1] using Skyrme forces is a versatile method for investigating many collective nuclear phenomena, such as heavy ion collisions [2, 3, 4, 5] and giant resonances [6, 7, 8]. It is an investigation of the latter, using TDHF, with which this paper is concerned. In particular, the focus is on giant magnetic dipole resonances. The main purpose is to investigate the effect that the tensor force present in the Skyrme interaction has on the prediction and reproduction of these resonances. Giant resonances in general, and magnetic dipole resonances in particular are often studied with methods derived from the Random Phase Approximation [9] or the Shell Model [10], with time-dependent methods giving a complementary picture. For the present purposes, ^{52}Cr ($Z=24$, $N=28$) has been chosen to allow easy comparison with experimental data [11, 12], as well as between assumptions in the form of the effective interaction, while being a spin-orbit unsaturated nucleus in which effects of the tensor interaction would not be masked.

2. Observed Strength

For the comparison of the presented calculations with data, two experiments are drawn upon: An older electron scattering experiment (which we refer to as ES) [11] and a newer

photon scattering experiment (referred to as PS) [12]. The ES data span excitations energies in ^{52}Cr between 7 and 12 MeV, while the PS data covers an excitation range 5 – 9.5 MeV. In the ES case, the multipolarity of resonances was not always unambiguous and we take those transitions assigned categories *A* and *B* in [11] as being of wholly or predominantly *M1* in character.

3. Theory

3.1. Skyrme Energy Density Functional

The calculations in this paper used the phenomenological Skyrme force. The two-body non-tensor and tensor parts of the full Skyrme force are given, respectively, by [14]

$$v_{12}^{(2)} = t_0(1 + x_0P_\sigma)\delta(\mathbf{r}_1 - \mathbf{r}_2) \quad (1)$$

$$+ \frac{t_1}{2}(1 + x_1P_\sigma)\left[\delta(\mathbf{r}_1 - \mathbf{r}_2)\mathbf{k}^2 + \mathbf{k}'^2\delta(\mathbf{r}_1 - \mathbf{r}_2)\right] \quad (2)$$

$$+ t_2(1 + x_2P_\sigma)\mathbf{k}' \cdot \delta(\mathbf{r}_1 - \mathbf{r}_2)\mathbf{k} \quad (3)$$

$$+ iW_0(\sigma_1 + \sigma_2) \cdot (\mathbf{k}' \times \delta(\mathbf{r}_1 - \mathbf{r}_2)\mathbf{k}) + \quad (4)$$

$$\frac{t_3}{6}(1 + x_3P_\sigma)\rho^\alpha\left(\frac{\mathbf{r}_1 + \mathbf{r}_2}{2}\right)\delta(\mathbf{r}_1 - \mathbf{r}_2) \quad (5)$$

$$v_t = \frac{t_e}{2}\left\{[3(\sigma_1 \cdot \mathbf{k}')(\sigma_2 \cdot \mathbf{k}') - (\sigma_1 \cdot \sigma_2)\mathbf{k}'^2]\delta(\mathbf{r}_1 - \mathbf{r}_2)\right. \\ \left.+ [3(\sigma_1 \cdot \mathbf{k})(\sigma_2 \cdot \mathbf{k}) - (\sigma_1 \cdot \sigma_2)\mathbf{k}^2]\delta(\mathbf{r}_1 - \mathbf{r}_2)\right\} \quad (6)$$

$$+ t_o\left\{[3(\sigma_1 \cdot \mathbf{k}')(\sigma_2 \cdot \mathbf{k}) - (\sigma_1 \cdot \sigma_2)\mathbf{k}' \cdot \mathbf{k}]\delta(\mathbf{r}_1 - \mathbf{r}_2)\right\}$$

where

$$\mathbf{k} = \frac{1}{2i}(\nabla_1 - \nabla_2) \quad \text{and} \quad \mathbf{k}' = -\frac{1}{2i}(\nabla'_1 - \nabla'_2) \quad (7)$$

$$\langle\phi|\mathbf{k}'|\phi\rangle = \int d^3r\phi^*\mathbf{k}'\phi = -\frac{1}{2i}\int d^3r[(\nabla_1 - \nabla_2)\phi^*]\phi \quad (8)$$

with \mathbf{k} acting to the right and \mathbf{k}' to the left.

There are many parameterisations of this force, fitted by different algorithms to varied sets of data and pseudodata. In the present work, SkM* [15], Sly5 [16], Sly5t [17], T12 [18] and T22 [18] are used in order to assess a widely-used force in which the tensor terms are inactive (SkM*), to compare a force which was originally fitted without the tensor terms (Sly5) to which tensor terms were later added without refitting the rest of the force (Sly5t) and forces which were fitted including the tensor terms (T12 and T14).

Using the Skyrme force, one can construct an energy density functional which, through a variational principle, can in turn be related to a single-particle Hamiltonian, which is then used to solve for the single-particle states. This can be used to create an

energy density functional of many gauge invariant quantities. In particular, we consider the effects of the following two gauge-invariant terms in the energy density functional:

$$\begin{aligned} & \frac{t_1 x_1 + t_2 x_2 - 2(t_e + t_o)}{8} \left(\mathbf{s}(r) \cdot \mathbf{T}(r) - \sum_{\mu\nu} J_{\mu\nu}(r)^2 \right) + \\ & \frac{t_2 - t_1 + 2(t_e - t_o)}{8} \sum_q \left(\mathbf{s}_q(r) \cdot \mathbf{T}_q(r) - \sum_{\mu\nu} J_{q,\mu\nu}(r)^2 \right) \end{aligned} \quad (9)$$

and

$$\begin{aligned} & \frac{3(t_e + t_o)}{4} \left(\mathbf{s}(r) \cdot \mathbf{F}(r) - \frac{1}{2} \sum_{\mu\nu} J_{\mu\nu}(r) J_{\nu\mu}(r) - \frac{1}{2} \sum_{\mu} J_{\mu\mu}(r)^2 \right) \\ & - \frac{3(t_e - t_o)}{4} \sum_q \left(\mathbf{s}_q(r) \cdot \mathbf{F}_q(r) - \frac{1}{2} \sum_{\mu\nu} J_{q,\mu\nu}(r) J_{q,\nu\mu}(r) - \frac{1}{2} \sum_{q\mu} J_{q,\mu\mu}(r)^2 \right), \end{aligned} \quad (10)$$

which we refer to as the $\mathbf{s} \cdot \mathbf{T}$ and $\mathbf{s} \cdot \mathbf{F}$ terms respectively.

A more thorough description the Skyrme energy density functional including the definitions of the densities given above and corresponding derivation of gauge invariant quantities is given in [19].

3.2. Hartree-Fock

In order to obtain the ground states from which to begin the time-dependent calculations, the *Sky3D* code [20] is used in static mode, with wave functions initialised as harmonic oscillator states, and iterated until self-consistent convergence.

3.3. Magnetic Dipole Resonances

The form of the magnetic dipole (M1) operator that has been used for this work is given by [21]

$$\begin{aligned} \hat{M}_{10} &= \mu_N \sum_{i=1}^A \left\{ g_s^{(i)} \hat{s}_i + g_l^{(i)} \hat{l}_i \right\} \cdot \left(\nabla r Y_{10}(x, y, z) \right)_{r=r_i} \\ Y_{10}(x, y, z) &= \frac{z}{r} \\ \hat{M}_{10} &= \mu_N \sum_{i=1}^A \left\{ g_s^{(i)} \hat{s}_i + g_l^{(i)} \hat{l}_i \right\} \cdot \left(\hat{z} \right)_{r=r_i} \\ \hat{M}_{10} &= \mu_N \sum_{i=1}^A \left\{ g_s^{(i)} \hat{s}_{z,i} + g_l^{(i)} \hat{l}_{z,i} \right\} \\ g_s^{(i)} &= g_p, \quad g_l^{(i)} = 1 \quad \text{for protons} \\ \text{and} \\ g_s^{(i)} &= g_n, \quad g_l^{(i)} = 0 \quad \text{for neutrons} \\ \hat{l}_{z,i} &= \frac{1}{i} \left(x \frac{d}{dy} - y \frac{d}{dx} \right) \end{aligned} \quad (11)$$

g_p and g_n are the g factors for the proton and neutron respectively, μ_N is the nuclear magneton, $s_{z,i}$ and $l_{z,i}$ are the spin and orbital z components respectively and Y_{10} is a

spherical harmonic. To see the effect of a magnetic transition, all frequencies of this transition can be excited at once using the following boost to the wavefunction

$$\psi_{new}(t=0) = e^{i\eta\hat{M}_{10}}\psi_{old}(t=0). \quad (12)$$

To keep within the linear response regime, a variable η is added to control the strength of the boost to the wavefunction. The expectation value of the operator M_{10} can be related to the strength function (the strength function gives prediction of how likely a transition is likely to occur for a given frequency or energy) associated with the transition, by [22]

$$S(E) = -\frac{1}{\pi\eta}\text{Im}(\mathcal{M}(\hbar\omega)). \quad (13)$$

in which \mathcal{M} is the fourier transform of the expectation value of M_{10} over time. This formula linking the strength function to expectation value in equation 13 is only valid within the linear regime.

4. Theoretical Results

4.1. Hartree-Fock Case Calculations

Hartree-Fock calculations were performed on a 3-dimensional Cartesian grid from -11.5 fm to $+11.5$ fm, in 1 fm steps in each direction. The above table outlines the properties of ^{52}Cr predicted in the static case for various Skyrme forces alongside known experimental data. The results produced are in relative agreement with experiment. The charge radius r_{rms} was approximately calculated from the nuclear proton radius r_{nucp} using the standard formula,

$$r_{rms}^2 = \langle r^2 \rangle_{nucp} + r_p^2, \quad (14)$$

with a value of the proton radius $r_p^2 = 0.64\text{fm}^2$ adopted from a recent review [27]

4.2. Sly5t and Sly5

The tensor force present in the Skyrme force has in the past been disregarded in many calculations as it is assumed to have a small effect compared to other terms in the

Force	B.E./A [MeV]	Charge Radius [fm]	β_2
Sly5	-8.427	3.708	0.157
Sly5t	-8.509	3.700	0.148
SKM*	-8.411	3.710	0.160
T12	-8.423	3.706	0.156
T22	-8.426	3.705	0.156
Experimental	-8.7762	3.643(3)	0.211

Table 1. Static (HF) output from Sky3D code, along with experimental results [24, 25, 26].

Force	Minimum Energy [MeV]	Maximum Energy [MeV]
Sly5	3.00	12.00
Sly5t	3.00	13.00
Sly5t SF OFF	3.00	12.50
Sly5t ST OFF	3.00	13.00
SKM*	2.50	11.50
T12	3.00	12.50
T22	3.00	12.50
Experimental	5.10	11.65

Table 2. Approximation of minimum and maximum energy of appreciable strength.

Skyrme force. Comparing the strength functions for Sly5 and Sly5t in figure 1, it can be seen that the effect of adding the tensor force is to redistribute the strength over a larger energy range. For example, the maximum energy where there is any appreciable strength is approximately 12 MeV, whereas for Sly5t this energy is approximately 13 MeV.

4.3. Instabilities

While performing the calculations in this paper, an instability was encountered. We suppose that this instability is due to the known problems in the spin orbit part of the Skyrme force [23]. We thus tested the version of the Sly5 which was adjusted to push the instability further away [23]. For ^{52}Cr it was found to be much more stable and allowed a higher resolution strength function to be produced. It should be noted, however, that for other nuclei, the instability still existed. The strength functions produced by this force are shown in figure 2.

4.4. Contribution of Different Galilean Invariant quantities

The particular combination of terms in the Skyrme interaction that give rise to gauge-invariant quantities may each be turned off or on as one chooses. Since some of these concern only time-odd quantities that are not fitted in the original definition of the forces, they are often set to zero for even for situations when they might otherwise be active, as is the case here. Therefore, the individual effects that these components (defined as the $\mathbf{s} \cdot \mathbf{T}$ and $\mathbf{s} \cdot \mathbf{F}$ terms, above) have on the strength function were investigated. The results with these terms turned on (Sly5t) or off (labelled in figure as “with ST term removed” etc) are shown in figure 1. The main result appears to be that the $\mathbf{s} \cdot \mathbf{F}$ term is responsible for a large part of the strength in the region around 8-10 MeV. There is considerable strength here from the full Sly5t force, which is much diminished by removal of the $\mathbf{s} \cdot \mathbf{F}$ term.

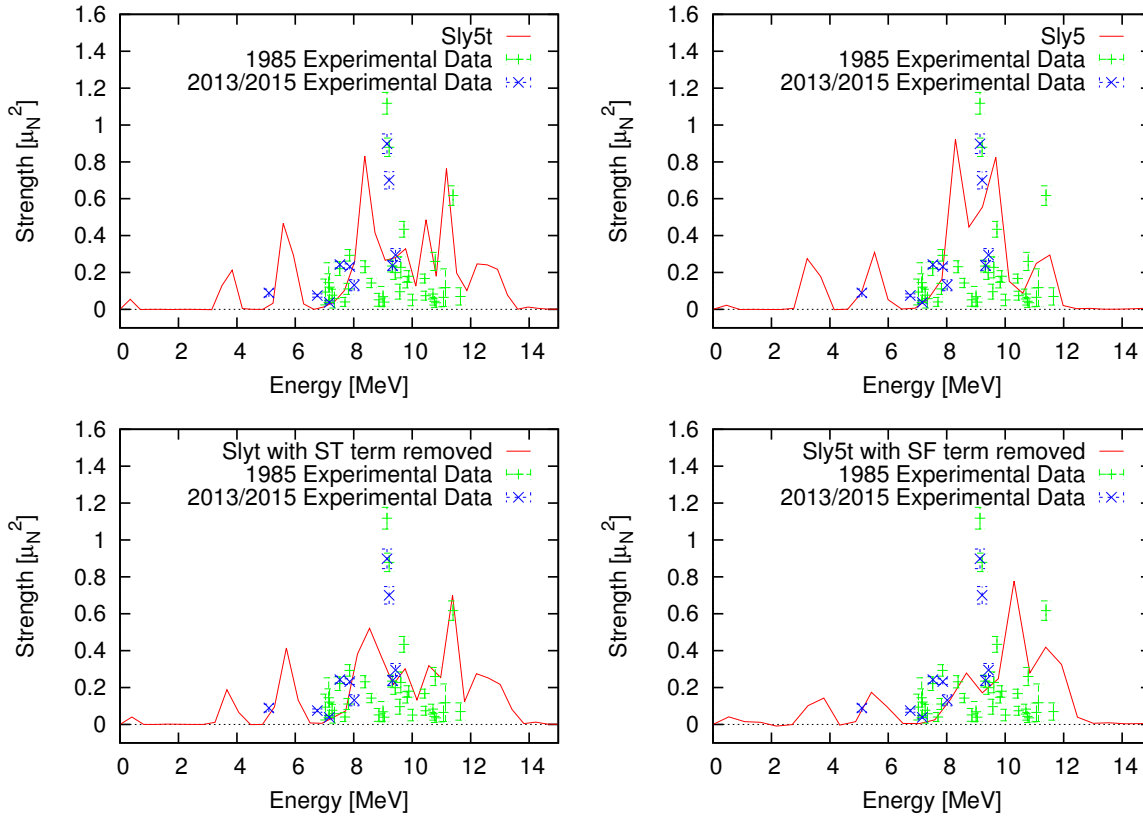


Figure 1. The strength functions for the Sly5 and Sly5t parameterisations of the Skyrme force. The strength functions for Sly5t with different Galilean invariant terms removed.

4.5. Different Skyrme forces

It was found that by changing the parameterisation of the force changed the distribution of the strength with the same energy region. The SKM* parameterisation appears to most closely replicate the energy region that has been experimentally been examined. The T12 and T22 parameterisations give similar strength functions. The resultant strength functions are shown in figure 2.

5. Conclusions

In conclusion it was found that the use of TDHF with Skyrme forces to model magnetic dipole transitions in the linear regime, at least in the case of ^{52}Cr is useful for predicting the range of energies which may initiate a magnetic dipole transition. An interesting thing to note is all the Skyrme forces predicting a transition at approximately 3 MeV, which presumably corresponds to a bound state. This study could be further expanded by looking at the recent experimental data for ^{50}Cr [29] or to expand the code to include higher order multipoles.

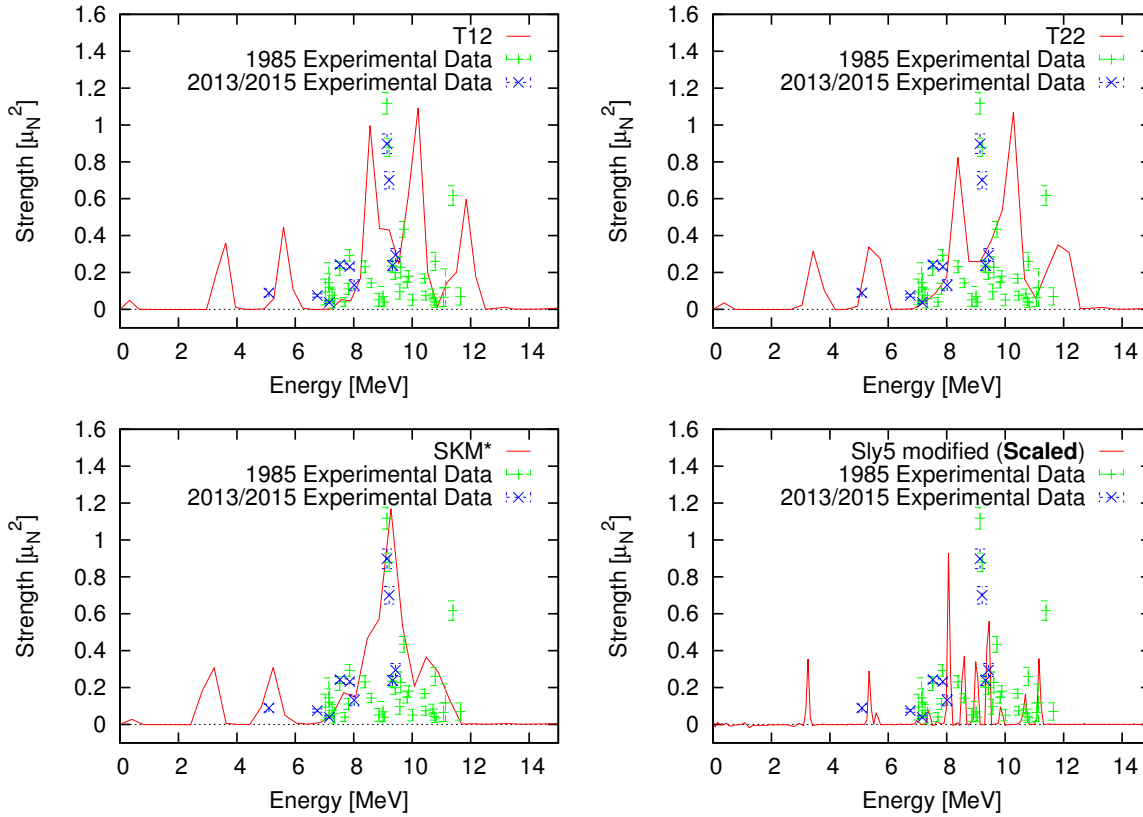


Figure 2. The strength functions produced for the parameterisations of the Skyrme force T12, T22 and SKM*, along with the modified version of Sly5 force designed to remove instabilities.

Acknowledgments

The authors gratefully acknowledge support from the UK Science and Technology Facilities Council (STFC) via awards ST/M503824/1 and ST/L005743/1 as well as computing time on the STFC DiRAC computer.

References

- [1] C. Simenel, *Eur. Phys. J. A* **48**, 152 (2012)
- [2] A. S. Umar, V. E. Oberacker, J. A. Maruhn, and P.-G. Reinhard, *Phys. Rev. C* **81**, 064607 (2010).
- [3] Kazuyuki Sekizawa and Kazuhiro Yabana, *Phys. Rev. C* **88**, 014614 (2013).
- [4] A. S. Umar and V. E. Oberacker, *Phys. Rev. C* **74**, 061601(R) (2006)
- [5] P. D. Stevenson, E. B. Suckling, S. Fracasso, M. C. Barton, A. S. Umar, [arXiv:1507.00645v1](https://arxiv.org/abs/1507.00645v1) (2015)
- [6] P. D. Stevenson, M. R. Strayer, J. Rikovska Stone, and W. G. Newton, *Int. J. Mod. Phys E* **13**, 181 (2004)
- [7] I. Stetcu, A. Bulgac, P. Magierski, and K. J. Roche, *Phys. Rev. C* **84**, 051309(R) (2011)
- [8] P. M. Goddard et. al, *Phys. Rev. C* **88**, 064308 (2013)
- [9] V. O. Nesterenko, et. al, *J. Phys. G: Nucl. Part. Phys.* **37**, 064034 (2010)
- [10] Kris Heyde, Peter von Neumann-Cosel, and Achim Richter, *Rev. Mod. Phys.* **82**, 2365 (2010)

- [11] D. I. Sober et al, *Phys. Rev. C* **31**, 2054 (1985)
- [12] Krishichayan, Megha Bhike, W. Tornow, G. Rusev, A. P. Tonchev, N. Tsoneva, and H. Lenske, *Phys. Rev. C* **91**, 044328 (2015)
- [13] Pai, H. et al., *Physical Review C*, **88**, 054316 (2013)
- [14] T. H. R. Skyrme *Nuclear Physics* **9** (1959) 615-634
- [15] J. Bartel et al., *Nucl. Phys.* **A386** 79-100 (1982)
- [16] E. Chabanat, et al., *Nucl. Phys.* **A627** 710-746 (1997)
- [17] G. Colò, et al, *Phys. Letts. B* **646** 227-231 (2007)
- [18] Lesinski, T. et al., *Phys. Rev. C* **76**, 014312 (2007)
- [19] Bender, M., Bennaceur, K., Duguet, T., Heenen, P.-H., Lesinski, T. and Meyer, J. *Phys. Rev. C* **80**, 064302 (2009)
- [20] Maruhn, J. A., Reinhard, P.-G, Stevenson, P. D., and Umar, A. S. *Comput. Phys. Commun.* **185**, 2195 (2014)
- [21] P. Ring and P. Schuck, *The Nuclear Many-Body Problem* Springer Verlag, Heidelberg (1980)
- [22] P. D. Stevenson and S. Fracasso *J. Phys. G: Nucl. Part. Phys.* **37**, 064030 (2010)
- [23] A. Pastore et al., *Physica Scripta* **T154**, 014014 (2013)
- [24] Lightbody, J. W. et al., *Phys. Rev. C* **27**, 113 (1983)
- [25] A.H. Wapstra and N.B. Gove, *At. Data Nucl. Data Tables*, **9**, 267 (1971)
- [26] *Chart of Nuclides National Nuclear Data Center*
- [27] Michael Bender, Paul-Henri Heenen, and Paul-Gerhard Reinhard, *Rev. Mod. Phys.* **75**, 121 (2003)
- [28] D. I. Sober, B. C. Metsch, W. Knpfer, G. Eulenberg, G. Kehler, A. Richter, E. Spamer, and W. Steffen, *Phys. Rev. C* **31**, 2054 (1985)
- [29] H. Pai, et al. *Phys. Rev. C* **93**, 014318 (2016)